

All-optical Polarization Phase Modulation in Coupled Quantum Dots

Ku Chul Je^{1,2} and Kwangseuk Kyhm^{1*}

¹*Department of Opto-mechatronics, Pusan National University, Busan 46287, Korea*
²*College of Liberal Arts and Sciences, Anyang University, Gyeonggi-do 14028, Korea*

(Received December 20, 2016 : revised January 2, 2017 : accepted January 3, 2017)

We have considered optical nonlinearities of coupled quantum dots theoretically, where an exciton dipole-dipole interaction is mediated between the adjacent large and small quantum dots. For increasing a pump pulse area in resonance with the large quantum dot exciton the induced nonlinear refractive index of the small quantum dot exciton has been obtained. As the exciton dipole-dipole interaction depends on the relative orientation of two exciton dipoles, the optical nonlinearities for the directions parallel and perpendicular to the coupling axis of the two quantum dots are compared. The directional imbalance of optical nonlinearities in coupled quantum dots can be utilized for a polarization phase modulator by controlling a pump pulse area and propagation length.

Keywords : Optical nonlinearities, Exciton, Polarization, Quantum dots
OCIS codes : (190.4720) Optical nonlinearities of condensed matter; (260.2130) Ellipsometry and polarimetry; (300.6240) Spectroscopy, coherent transient

I. INTRODUCTION

During the last decade, coupled quantum dots (CQDs) have been of great interest to study the quantum nature of superposition and entanglement [1-6]. This can be realized by stacking quantum dots (QDs) vertically with a barrier layer, where the QDs are grown by the Stranski-Krastanov growth method. Also, when QDs are formed by the interface fluctuation of a quantum well thickness, laterally neighbored QDs can be found. Likewise, laterally coupled QD structures can also be generated when dense colloidal QDs are dispersed [8, 9]. Additionally, the droplet epitaxy method enables control of the morphology of laterally-coupled QD structures [4, 5].

When the size of the two QDs are different, an energy resonance can be induced by applying an external DC-electric field, resulting in a wavefunction overlap between the QDs via the tunneling effect [6]. In this case, the tunneling effect is limited by a short inter-dot distance (<10 nm). On the other hand, the exciton dipole-dipole interaction can be utilized as an alternative method of inter-dot coupling [7]. As it is based on the Coulomb inter-

action, the exciton dipole-dipole interaction still works at relatively long distance. As the dipole-dipole interaction depends on the dipole orientation, interaction between the two QDs can be controlled selectively by optical polarization direction. The DC-electric control needs extra fabrication processes for electrodes, and the resonance condition also depends on the QD size difference. However, the exciton dipole-dipole interaction still works with an energy tolerance among size different QDs, and no extra fabrication is necessary for electrodes in the case of DC-electric control. Therefore, optical control of CQDs is feasible for a practical device and also applicable to inhomogeneous QD ensembles.

In this work, we calculated polarization dependence of optical nonlinearities in lateral CQDs, where the nonlinear refractive indices between the direction parallel and perpendicular to the QD coupled axis are imbalanced as a consequence of the directional dependence of the exciton dipole-dipole interaction.

*Corresponding author: kskyhm@pusan.ac.kr

Color versions of one or more of the figures in this paper are available online.



This is an Open Access article distributed under the terms of the Creative Commons Attribution Non-Commercial License (<http://creativecommons.org/licenses/by-nc/4.0/>) which permits unrestricted non-commercial use, distribution, and reproduction in any medium, provided the original work is properly cited.

II. METHODS

As shown in Fig. 1, we considered two neighboring spherical QDs, where the surface-to-surface distance ($d = 15\text{\AA}$) and the radii of small ($R_A = 30\text{\AA}$) and large ($R_B = 30.5\text{\AA}$) QDs are given. In a practical point of view, this can be easily found in size distributed colloidal QDs. Therefore, we considered CdSe colloidal QDs as a feasible example, but this model can also be utilized for a lateral CQD grown by droplet epitaxy. In the case of a CdSe QD, the exciton ground state is the 1^L bright fine state [8, 10-13].

Although the size difference is small, the energy difference between the two ground exciton states of small (X_A) and large (X_B) QDs is ~ 14 meV. Nevertheless, the exciton dipole-dipole interaction is still effective in the presence of the energy difference between X_A and X_B . Suppose a single CQD structure is well isolated, this can be analogous to the atomic three-level system in quantum optics, where electrically induced transparency is studied. However, the origin of optical nonlinearities is different. While an exciting light pulse is resonant with X_B , the refractive index of X_A also changes through the exciton dipole-dipole interaction. For increasing the exciting pulse intensity, the

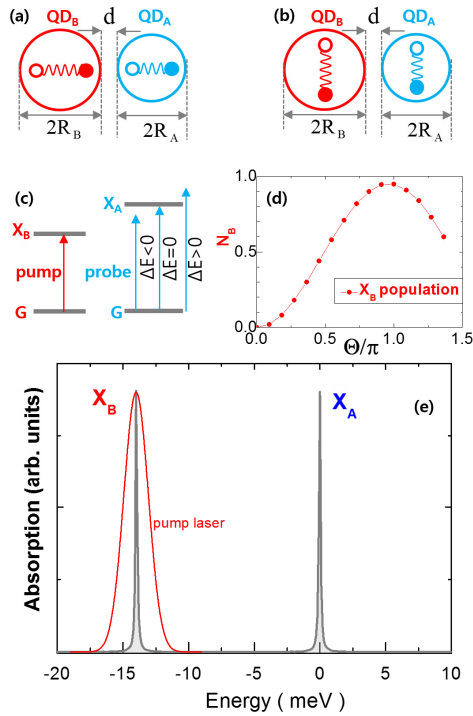


FIG. 1. Schematic diagram of coupled quantum dots when the excitons of large (QD_A) and small (QD_B) quantum dots are parallel (a) or perpendicular (b) to the coupling direction. With increasing a pump pulse area, which is in resonance with QD_A energy (c,e), the enhanced exciton population at QD_A (d) gives rise to a transient optical nonlinearity of the detuned ($\Delta E < 0$ and $\Delta E > 0$) and resonant ($\Delta E = 0$) probe.

occupancy of both X_A and X_B are increased. Therefore, the exciton dipole-dipole interaction also depends on the exciton occupancy. In this case, the Coulomb interaction needs to be considered carefully by considering the exciton occupancy.

Additionally, it is noticeable that the exciton dipole-dipole interaction depends on the relative orientation of two exciton dipoles. For the orientation dependence of a pair of dipoles, two cases were compared, i.e., X_A and X_B are parallel (Fig. 1(a)) or perpendicular (Fig. 1(b)) to the QD coupled direction, which is denoted by H-polarized and V-polarized, respectively.

The Hamiltonian can be given by $H = H_{QD} + V_C$, where H_{QD} is the energy of X_A and X_B and the dipole radiation associated with by a light pulse, and V_C describes the Coulomb interaction between X_A and X_B [7, 14]. More specifically, H_{QD} is given by

$$\begin{aligned}
 H_{QD} = & \sum_{\lambda_A} (\hbar\omega_{\lambda_A}^e \alpha_{\lambda_A}^\dagger \alpha_{\lambda_A} + \hbar\omega_{\lambda_A}^h \beta_{\lambda_A}^\dagger \beta_{\lambda_A}) \\
 & + \sum_{\lambda_B} (\hbar\omega_{\lambda_B}^e \alpha_{\lambda_B}^\dagger \alpha_{\lambda_B} + \hbar\omega_{\lambda_B}^h \beta_{\lambda_B}^\dagger \beta_{\lambda_B}) \\
 & - E(t) \sum_{\lambda_A} (d_{\lambda_A} \alpha_{\lambda_A}^\dagger \beta_{\lambda_A}^\dagger + c.c.) \\
 & - E(t) \sum_{\lambda_B} (d_{\lambda_B} \alpha_{\lambda_B}^\dagger \beta_{\lambda_B}^\dagger + c.c.)
 \end{aligned} \quad (1)$$

For QD_A , $\hbar\omega_{\lambda_A}^{e(h)}$ is the energy of an electron (hole) in the exciton state λ , which is either H-polarized or V-polarized excited exciton state and an unexcited state. $\alpha_{\lambda_A}^\dagger$ (α_{λ_A}) and $\beta_{\lambda_A}^\dagger$ (β_{λ_A}) are the creation (annihilation) operators for electrons and holes. $E(t)$ and d_{λ_A} are the amplitude of a pump pulse (~ 1 ps) and the interband optical transition matrix element, respectively. Therefore, V_C can be described by

$$\sum_{\lambda_A} V_{\lambda_A, \lambda_B} (\alpha_{\lambda_A}^\dagger \alpha_{\lambda_A} + \beta_{\lambda_A}^\dagger \beta_{\lambda_A}) (\alpha_{\lambda_B}^\dagger \alpha_{\lambda_B} + \beta_{\lambda_B}^\dagger \beta_{\lambda_B}) \quad (2)$$

where observable quantities can be defined such as the interband transition $\langle \beta_{\lambda_i} \alpha_{\lambda_i} \rangle = p_{\lambda_i}(t)$, the electron (hole) occupancy $\langle \alpha_{\lambda_A}^\dagger \alpha_{\lambda_A} \rangle$ ($\langle \beta_{\lambda_A}^\dagger \beta_{\lambda_A} \rangle$) = N_{e, λ_i} (N_{h, λ_i}), and the total polarization $P_{tot}(t) = \sum_i P_i(t) = \sum_{\lambda_i} p_{\lambda_i}(t)$.

The equations of motion for those observable quantities are described by the semiconductor Bloch equations as [15, 16]

$$\frac{d}{dt} p_{\lambda_A(B)} = -i \left(\omega_{\lambda_A(B)} + \sum V_{eh, \lambda_A(B)} N_{\lambda_{B(A)}} \right) p_{\lambda_A(B)} \quad (3)$$

$$\frac{d}{dt} N_{\lambda_A(B)} = -2Im \left(\frac{d_{\lambda_A(B)} E(t)}{\hbar} p_{\lambda_A(B)}^* \right) \quad (4)$$

whereby the nonlinear refractive index spectrum $\tilde{n}(\omega, N(\Theta)) = n(\omega, N(\Theta)) + ik(\omega, N(\Theta))$ can be obtained.

III. RESULTS AND DISCUSSION

As shown in Fig. 1(d), the occupancy of X_B is increased gradually with increasing a pump pulse area Θ , which becomes maximized at $\Theta = \pi$. For an isolated QD, we have already calculated the refractive index change, where the real and imaginary parts of the refractive index spectrum were shown for pump intensity ($\sim \Theta^2$) [15]. Although the exciton dipole-dipole interaction has been well known in terms of resonance energy transfer (FRET), its nonlinearity is barely considered. However, as shown schematically in Fig. 1(c), the optical nonlinearity of X_A can appear through the exciton dipole-dipole interaction as N_B increases. Since it depends on a frequency difference with respect to its resonance as shown schematically in Fig. 1(c), we calculated the real and imaginary parts of the nonlinear refractive index spectrum near the X_A energy under resonant excitation of X_B .

Figure 2(a) and (b) show the real ($n(\omega, \Theta)$) and imaginary ($\kappa(\omega, \Theta)$) parts of the nonlinear refractive index spectrum for the H-polarized excitation. As Θ is increased, a spectral splitting is seen in the $n(\omega, \Theta)$ and $\kappa(\omega, \Theta)$ spectrum, which is a distinguishing feature of the dipole-dipole interaction compared to the results of an isolated QD. This result reminds us of the spectral splitting of dressed states as a consequence of light-matter interaction. For example, a spectral splitting of the emitter in a cavity appears as the cavity field becomes strongly coupled with the emitter, and recently the cavity field can be replaced with the strong local surface plasmon of a metal nanostructure. In this sense, the nonlinear exciton dipole-dipole interaction is quite similar, and the spectral splitting indicates a degree of the nonlinear coupling between two exciton dipoles.

From a practical point of view, a pulse laser is necessary to induce transient optical nonlinearities, and the preferential direction of the exciton dipole-dipole interaction can be selected by the pump pulse polarization. However, the energy difference (a few meV) between the H- and V-polarized states of an exciton pair is vulnerable to thermal transition. Therefore, both the H- and V-polarized states contribute to the optical nonlinearities. As shown in Fig. 2(c) and (d), the nonlinear spectrum for the V-polarized excitation are different from those for the H-polarized exciton pair due to the directional dependence of the exciton dipole-dipole interaction. Suppose the transient optical nonlinearities are utilized for all-optical phase modulation, the imbalanced nonlinear refractive index between the H- and V-polarized should be considered.

In Fig. 3, the changes of the nonlinear refractive index with respect to the linear refractive index, i.e. $\Delta n(\omega, \Theta) = n(\omega, \Theta > 0) - n(\omega, \Theta = 0)$ and $\Delta \kappa(\omega, \Theta) = \kappa(\omega, \Theta > 0) - \kappa(\omega, \Theta = 0)$, are shown at negative-detuned ($\Delta E = -0.1$ meV) (a), resonant ($\Delta E = 0$) (b), and positive-detuned ($\Delta E = +0.1$ meV) (c) probe light for the H- and V-polarized exciton pairs, respectively. When the probe light is resonant ($\Delta E = 0$), both the H- and V-polarized excitons are similar in the real

part change of the nonlinear refractive index $\Delta n_{\text{HK}} \approx \Delta n_V$. On the other hand, a significant difference is shown in the imaginary part change. Therefore, the incident linear polarization of a probe light barely rotates, but the ellipticity becomes enhanced. For the positive- and negative detuned

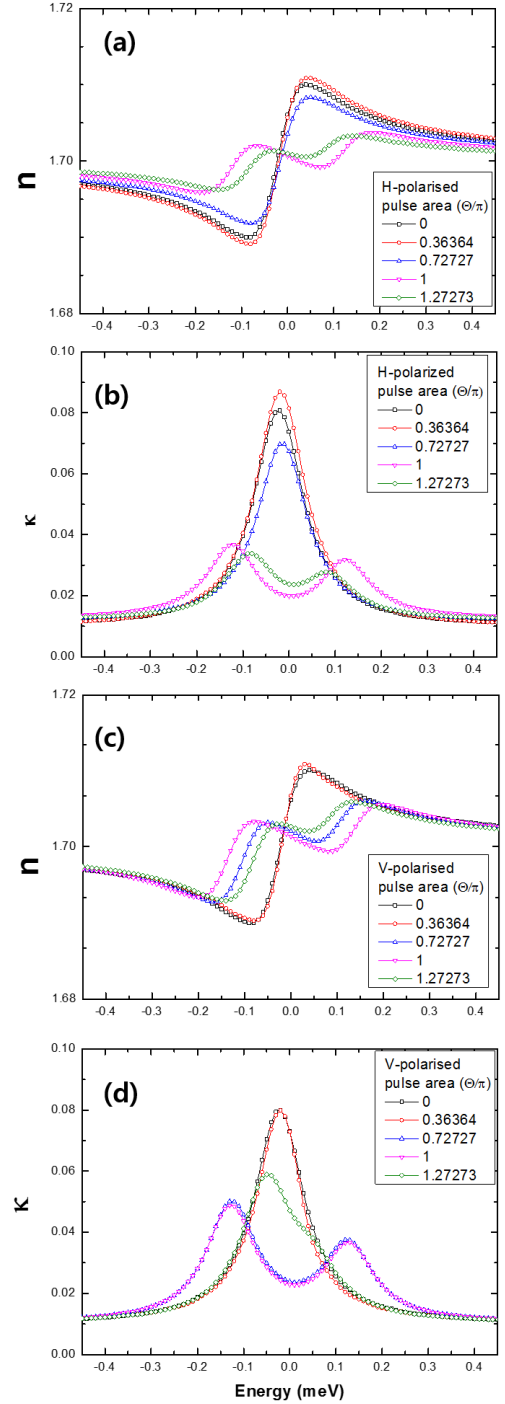


FIG. 2. The real (n) (a, c) and imaginary (κ) (b, d) refractive index spectrum of X_A for increasing the pump pulse area (Θ) resonant to the QD_B exciton energy, where the polarization of a pump pulse is either parallel (H-polarized) or perpendicular (V-polarized) to the QD coupling direction.

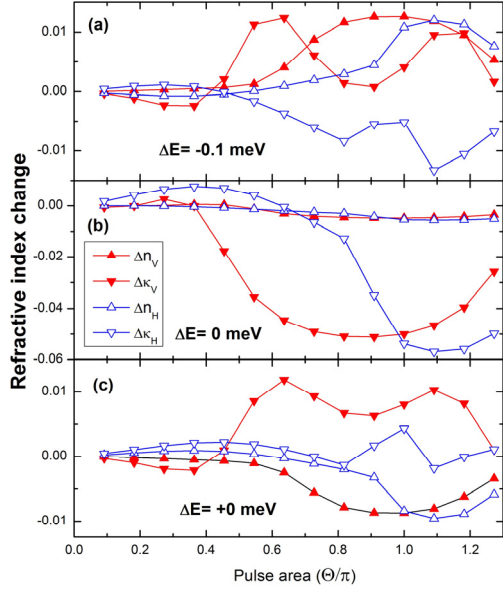


FIG. 3. Refractive index change in real (Δn) and imaginary ($\Delta \kappa$) parts for increasing either H or V-polarized pulse area (Θ) resonant with the QD_B exciton when the probe energy is below (a), resonant (b), and above (c) the QD_A exciton.

probes, the pump pulse area should be large enough ($\Theta > 0.4\pi$) to observe a significant polarization modulation. In experimental point of view, this implies more than 16% of the exciton saturation intensity is necessary.

When the imbalanced optical nonlinearities of the H- and V-polarized exciton are utilized for a practical all-optical polarization modulation, a precise phase modulation needs to be predicted. As an example, we have considered the modulated polarization of the negative detuned probe ($\Delta E = -0.1$ meV), the modulated polarization can be represented in terms of rotational (θ) and elliptical (ϵ) angles as shown in Fig. 4(b). Given the refractive index change of X_A induced by pumping X_B with a pulse area (Θ), the modulated polarization Jones vector (\tilde{E}_x , \tilde{E}_y) can be described as

$$\begin{bmatrix} \tilde{E}_x \\ \tilde{E}_y \end{bmatrix} = \begin{bmatrix} E_0 \exp\left(-\frac{\omega}{c} \kappa_{HZ}\right) \exp\left(i \frac{\omega}{c} n_{HZ}\right) \\ E_0 \exp\left(-\frac{\omega}{c} \kappa_{VZ}\right) \exp\left(i \frac{\omega}{c} n_{VZ}\right) \end{bmatrix} \quad (5)$$

$$= \begin{bmatrix} |\tilde{E}_x| e^{i\phi_x} \\ |\tilde{E}_y| e^{i\phi_y} \end{bmatrix} \quad (6)$$

where the amplitude of an incident probe light and the induced phase components are denoted by E_0 and $\phi_{x,y}$, respectively. Regarding the density of QDs in a feasible device, we assume $\frac{\omega z}{c} = \frac{2\pi z}{\lambda} \sim 100$. This implies the propagation length $z \sim 10\mu\text{m}$ with a multiple QD layers. Elliptical polarization states can also be characterized by

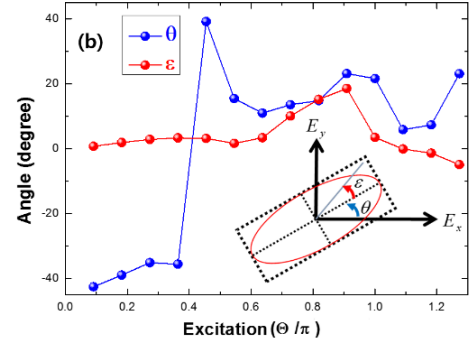
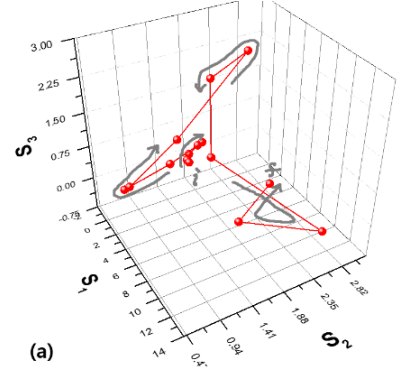


FIG. 4. For increasing the excitation of a pump pulse area (Θ), the linear polarization of a probe, which is off-resonant ($\Delta E = -0.1$ meV) to X_A exciton, becomes elliptically polarized due to the phase retardation arising from the imbalanced transient optical nonlinearity between the H- (denoted by x) and V-polarized (y) direction. The elliptical polarization for excitation is mapped into the Poincaré sphere (a) and characterized in terms of rotational (θ) and elliptical angles (ϵ) (b).

using Stokes parameters as

$$S_0 = |\tilde{E}_x|^2 + |\tilde{E}_y|^2, \quad (7)$$

$$S_1 = |\tilde{E}_x|^2 - |\tilde{E}_y|^2, \quad (8)$$

$$S_2 = 2|\tilde{E}_x||\tilde{E}_y|\cos(\phi_x - \phi_y), \quad (9)$$

$$S_3 = -2|\tilde{E}_x||\tilde{E}_y|\sin(\phi_x - \phi_y), \quad (10)$$

whereby the elliptical (ϵ) and rotational (θ) angles can be obtained as

$$\theta = \frac{1}{2} \tan^{-1} \left(\frac{s_2}{s_1} \right) \quad (11)$$

$$\epsilon = \frac{1}{2} \sin^{-1} \left(\frac{s_3}{s_0} \right) \quad (12)$$

In Fig. 4(a), the polarization state for increasing excitation pulse area (Θ) is mapped in the normalized Poincaré sphere, which enables to overview the degree of linearity and ellipticity. Fig. 4(b) also shows $\epsilon(\Theta)$ and $\theta(\Theta)$. Interestingly, remains near zero whilst increases. Therefore, this low pulse area range ($\Theta < 0.5\pi$) can be utilized for rotational polarization control similar to the Faraday rotator. On the other hand, the ellipticity becomes significant when $0.5\pi < \Theta < \pi$. This range is useful as a waveplate by extending the propagation length. Consequently, a precise phase modulation can be realized by excitation and propagation length.

V. CONCLUSION

In conclusion, we have proposed that coupled quantum dots can be utilized as an all-optical polarization phase modulator. When an exciton dipole-dipole interaction is present between the size different two quantum dots, resonant excitation to the large quantum dot gives rise to optical nonlinearities of the small quantum dot. As the induced optical nonlinearities depend on the orientation of an exciton pair, a modulated polarization phase can be controlled in terms of excitation and propagation length.

ACKNOWLEDGMENT

This work was supported by a 2-year research Grant of Pusan National University (2015. 3. 1 ~ 2017. 2. 28).

REFERENCES

1. M. Bayer, P. Hawrylak, K. Hinzer, S. Fafard, M. Korkushinski, Z. R. Wasilewski, O. Stern, and A. Forchel, "Coupling and entangling of quantum states in quantum dot molecules" *Science* **291**, 451 (2001)
2. W. Sheng and J. Leburton, "Spontaneous localization in InAs/GaAs self-assembled quantum dot molecules" *Applied Rev. Lett.* **81**, 4449 (2002)
3. G. Bester, J. Shumway, and J. Zunger, "Theory of excitonic spectra and entanglement engineering in dot molecules" *Phys. Rev. Lett.* **93**, 047401 (2004)
4. X. R. Zhou, J. H. Lee, G. J. Salamo, M. Royo, M. Climente, and M. Doty, "Coulomb interaction signatures in self-assembled lateral quantum dot molecules" *Phys. Rev. B* **87**, 125309 (2013).
5. M. F. Doty, J. I. Climente, M. Korkushinski, M. Scheibner, A. Bracker, P. Hawrylak, and D. Gammon, "Antibonding ground states in InAs quantum dot molecules" *Phys. Rev. Lett.* **102**, 047401 (2009).
6. L. Wang, A. Rastelli, S. Kiravittaya, M. Benyoucef, and O. G. Schmidt, "Self-assembled quantum dot molecules" *Adv. Mater.* **21**, 2601 (2009).
7. T. Unold, K. Mueller, C. Lienau, T. Elsaesser, and A. D. Wieck, "Optical control of excitons in a pair of quantum dots coupled by the dipole-dipole interaction" *Phys. Rev. Lett.* **94**, 137404 (2005).
8. Victor I. Klimov, *Semiconductor and Metal Nanocrystals* (Marcel Dekker, Inc., New York- Basel, 2004).
9. H. Htoon, S. A. Crooker, M. Furis, S. Jeong, Al. L. Efros, and V. I. Klimov, "Anomalous circular polarization of photoluminescence spectra of individual CdSe nanocrystals in an applied magnetic field" *Phys. Rev. Lett.* **102**, 017402 (2009).
10. M. Furis, H. Htoon, M. A. Petruska, V. I. Klimov, T. Barrick, and S. A. Crooker, "Bright-exciton fine structure and anisotropic exchange in CdSe nanocrystal quantum dots" *Phys. Rev. B* **73**, 241313(R) (2006).
11. H. Htoon, M. Furis, S. A. Crooker, S. Jeong, and V. I. Klimov, "Linearly polarized fine structure of the bright exciton state in individual CdSe nanocrystal quantum dots" *Phys. Rev. B* **77**, 035328 (2008).
12. D. J. Norris, Al. L. Efros, M. Rosen, M. G. Bawendi, *Phys. Rev. B* **53**, 16347 (1996).
13. Al. L. Efros, M. Rosen, M. Kuno, M. Nirmal, D. J. Norris, and M. G. Bawendi, "Size dependence of exciton fine structure in CdSe quantum dots" *Phys. Rev. B* **54**, 4843 (1996).
14. K. C. Je, "Optical excitonic absorption spectrum in coupled quantum dots due to dipole-dipole interactions" *J. Kor. Phys. Soc.* **67**, 896 (2015).
15. K. C. Je, I. C. Shin, J. H. Kim, and K. S. Kyhm, "Surface-plasmon-assisted modal gain enhancement in Au-hybrid CdSe/ZnS nanocrystal quantum dots" *Appl. Phys. Lett.* **97**, 103110 (2010).
16. H. Haug and S. W. Koch, *Quantum theory of the optical and electric properties of semiconductors*, 4th Edition (World Scientific, Singapore, 2004)